THE JOURNAL OF BIOLOGICAL CHEMISTRY VOL. 286, NO. 9, pp. 7468–7478, March 4, 2011

FoxO Transcription Factors Promote Cardiomyocyte Survival upon Induction of Oxidative Stress*

Received for publication, August 26, 2010, and in revised form, December 8, 2010 Published, JBC Papers in Press, December 15, 2010, DOI 10.1074/jbc.M110.179242

Arunima Sengupta[‡], **Jeffery D. Molkentin**[‡], **Ji-Hye Paik**[§], **Ronald A. DePinho**[§], **and Katherine E. Yutzey**[‡1]

From the [‡]*Heart Institute, Division of Molecular Cardiovascular Biology, Cincinnati Children's Medical Center, Cincinnati, Ohio 45229 and the* [§]*Departments of Medical Oncology, Medicine, and Genetics, Belfer Institute for Applied Cancer Science, Dana Farber Cancer Institute, Harvard Medical School, Boston, Massachusetts 02115*

Transcriptional regulatory mechanisms of cardiac oxidative stress resistance are not well defined. FoxO transcription factors are critical mediators of oxidative stress resistance in multiple cell types, but cardioprotective functions have not been reported previously. FoxO function in oxidative stress resistance was investigated in cultured cardiomyocytes and in mice with cardiomyocyte-specific combined deficiency of FoxO1 and FoxO3 subjected to myocardial infarction (MI) or acute ischemia/reperfusion (I/R) injury. Induction of oxidative stress in cardiomyocytes promotes FoxO1 and FoxO3 nuclear localization and target gene activation. Infection of cardiomyocytes with a dominant-negative FoxO1(Δ256) adenovirus results in a significant increase in reactive oxygen species and cell death, whereas increased FoxO1 or FoxO3 expression reduces reactive oxygen species and cell death. Mice generated with combined conditional deletion of FoxO1 and FoxO3 specifically in cardiomyocytes were subjected to I/R or MI. Loss of FoxO1 and FoxO3 in cardiomyocytes results in a significant increase in infarct area with decreased expression of the antiapoptotic molecules, PTEN-induced kinase1 (PINK1) and CBP/P300-interacting transactivator (CITED2). Expressions of the antioxidants catalase and manganese superoxide dismutase-2 (SOD2) and the autophagy-related proteins LC3II and Gabarapl1 also are decreased following I/R compared with controls. Mice with cardiomyocyte-specific FoxO deficiency subjected to MI have reduced cardiac function, increased scar formation, induction of stress-responsive signaling, and increased apoptotic cell death relative to controls. These data support a critical role for FoxOs in promoting cardiomyocyte survival during conditions of oxidative stress through induction of antioxidants and cell survival pathways.

Ischemic heart disease or myocardial ischemia/reperfusion (I/R)[2] injury is a leading cause of mortality worldwide (1). Cardiac oxidative injury can lead to cardiomyocyte cell death followed by fibrosis, hypertrophy, ventricular chamber dilation, decreased cardiac function, and ultimately heart failure. Oxidative stress is associated with increased formation of reactive oxygen species (ROS) that contribute to the pathophysiology of I/R injury (1). Increased ROS leads to DNA, protein and lipid modifications, as well as activates stress-signaling pathways leading to heart failure in I/R injury (2). Protective factors in ROS-mediated cardiac injury include AMP-activated protein kinase (AMPK) and sirtuins (Sirts) (3, 4). Understanding the intracellular processes that protect the heart from oxidative damage following I/R injury is important for the development of therapies to prevent the progression of heart disease.

FoxO transcription factors (FoxO1, FoxO3, FoxO4, and FoxO6) belong to the forkhead family of transcriptional regulators, of which FoxO1 and FoxO3 are expressed in developing and adult cardiomyocytes (5, 6). Mice lacking FoxO1 are embryonic lethal by E10.5 due to impaired vasculogenesis, and mice lacking FoxO3 are viable but develop a mild hemolytic anemia and premature ovarian failure as well as cardiac hypertrophy as adults (7–9). During the neonatal period, FoxOs promote neonatal cell cycle withdrawal through activation of cell cycle inhibitor genes $p21^{CIP1}$ and $p27^{KIP1}$ (5). FoxOs also function in cardiomyocyte cell size regulation through induction of autophagy and inhibition of hypertrophy (6, 9). In multiple cell types, FoxOs have a protective role in resistance to oxidative stress through regulation of antioxidant genes *SOD2* and catalase (*Cat*) as well as additional cell survival pathways (10). Importantly, FoxO interacting pathways and downstream targets responsible for oxidative stress resistance are highly context- and cell lineage-dependent (11). Under conditions of starvation or oxidative stress, FoxOs can be activated by increased AMPK activity or decreased activity of AKT (10). However, the specific functions of FoxOs in protection from I/R injury in the heart are not well understood.

FoxO1 and FoxO3 are co-expressed in cardiomyocytes and are coordinately regulated during neonatal cell cycle withdrawal or under starvation conditions (5, 6). Here, we demonstrate that FoxO1 and FoxO3 are both induced and protect cultured cardiomyocytes from oxidative injury. Likewise, combined deficiency of FoxO1 and FoxO3 specifically in cardiomyocytes in mice leads to increased oxidative damage and decreased myocardial function after acute I/R injury or myocardial infarction (MI).

* This work was supported, in whole or in part, by National Institutes of Health Grant PO1 HL069779 (to K. E. Y. and J. D. M.).

[1] To whom correspondence should be addressed: Division of Molecular Cardiovascular Biology, Cincinnati Children's Medical Center ML 7020, 240 Albert Sabin Way, Cincinnati, OH 45229. Tel.: 513-636-8340; Fax: 513-636-5958; E-mail: katherine.yutzey@cchmc.org.

[2] The abbreviations used are: I/R, ischemia/reperfusion; MI, myocardial infarction; ROS, reactive oxygen species; AMPK, AMP-activated protein kinase; 8-OHdG, 8-hydroxy-2′-deoxyguanosine; H/R, hypoxia/reoxygenation; qRT, quantitative real time; AAR, area at risk.

EXPERIMENTAL PROCEDURES

Neonatal Rat Cardiomyocyte Isolation and Culture—Primary neonatal rat cardiomyocytes were isolated from hearts of 1–2-day-old Sprague-Dawley rat pups as described previously (12). After separation from fibroblasts, enriched cardiomyocytes were plated on 2-well chamber slides for immunofluorescence or on 10-cm diameter dishes for Western blot or chromatin immunoprecipitation (ChIP) experiments. Cells were grown in DMEM (10-017-CV, Cellgro) containing 10% fetal bovine serum (FBS) and 1× penicillin/streptomycin (Invitrogen).

Induction of Oxidative Stress by Glucose-free Hypoxia and Reoxygenation (H/R) or Hydrogen Peroxide Treatment—Hypoxic oxidative stress was induced in neonatal cardiomyocytes by incubation in an anaerobic container that contained an Anaero Pack (Mitsubishi Gas Chemical) according to the manufacturer's instructions (13). The percent O_2 in the jar after 2 h with the Anaero Pack is 0%. DMEM/FBS-containing medium was replaced with glucose-free DMEM before the cells were exposed to hypoxic stress overnight, followed by 5 h of reoxygenation in medium with 10% FBS-containing DMEM (reoxygenation medium). For the normoxic condition, cardiomyocytes were incubated with DMEM/FBS/glucose-containing medium. Neonatal cardiomyocytes were treated with H_2O_2 (50 μM) for 2 h to induce oxidative stress and then either harvested for protein isolation and ROS measurement or processed for immunohistochemistry. FoxO1 and FoxO3 proteins were detected using antibodies from Millipore (AB4130) and Upstate (07-702), respectively. In some experiments, cells were infected with adenovirus for 24 h as described previously prior to the induction of oxidative stress (6). Wild type (WT), constitutively active (ADA), and dominant-negative (Δ256) FoxO1 adenoviruses were obtained from D. Accili (see Ref. 14). WT and constitutively active (TmO3) FoxO3 were obtained from K. Walsh (see Ref. 15). Infection with CMV β-galactosidase (β-gal) virus was used as a control for all experiments.

Measurement of ROS—Neonatal cardiomyocytes were incubated with 2′,7′-dichlorodihydrofluorescein diacetate (20 μM, Invitrogen) for 30 min at 37 °C in the dark (16). Cells were then incubated without or with H_2O_2 for 30 min, washed with PBS to eliminate the excess 2′,7′-dichlorodihydrofluorescein diacetate, and harvested in PBS containing 0.2% Triton X-100. Formation of ROS was detected by measuring the fluorescence absorbance (485-nm excitation and 530-nm emission) by a plate reader (BioTek, Flx800). Statistical analyses were performed using Student's *t* test ($p < 0.05$).

Animal Models—All experimental procedures with animals were approved by the Institutional Animal Care and Use Committee of the Cincinnati Children's Hospital Medical Center. FoxO1-LoxP-targeted (*FoxO1*$^{fl/fl}$) and FoxO3-LoxP-targeted (*FoxO3*$^{fl/fl}$) mice have been used previously for conditional Cre-dependent loss of FoxO1 and FoxO3 (11). *FoxO1*$^{fl/fl}$ and *FoxO1*$^{fl/fl}$ mice were crossed with each other to generate *FoxO1*$^{fl/fl}$/*FoxO3*$^{fl/fl}$ mice. *FoxO1*$^{fl/fl}$/*FoxO3*$^{fl/fl}$ mice were crossed with cardiac-specific *βMHC-Cre* transgenic mice to conditionally delete both FoxO1 and FoxO3 specifically from cardiomyocytes (17). All mice are in an FVBN background. For all studies, cardiomyocyte-specific FoxO1/FoxO3-deficient mice (*βMHC-Cre*;*FoxO1*$^{fl/fl}$/*FoxO3*$^{fl/fl}$) were compared with age-matched littermate control mice (*FoxO1*$^{fl/fl}$/*FoxO3*$^{fl/fl}$).

I/R and MI in Mice—Cardiac ischemia-reperfusion injury was performed in 8–10-week-old mice as described previously (18). Briefly, mice were anesthetized with 0.5% isoflurane in 95% O_2, 5% CO_2. Ischemia was achieved using an 8-0 prolene suture around the left anterior descending coronary artery and tied with a slipknot. The thoracotomy was closed, and the mice were revived for a 1-h ischemic injury period, after which the knot was released and the heart was allowed to reperfuse for 24 h. After reperfusion, mice were sacrificed by CO_2 asphyxiation, and 2% Evan's blue dye was injected into the left ventricle. Hearts were embedded in 2% agarose phosphate-buffered saline, sectioned in 2–3-mm slices, and stained with 2% triphenyltetrazolium chloride in saline overnight. Images of each slice were captured and analyzed to identify area at risk, infarct area, and viable myocardium. Alternatively, mice subjected to I/R were sacrificed by CO_2 asphyxiation, and hearts were harvested for RNA and protein isolation. The MI procedure was identical except that the ligature was permanent with no reperfusion, and mice were kept for 4 weeks. Trans-thoracic echocardiography was performed each week for 4 weeks to determine the cardiac ventricular performance and chamber dimensions as described previously (19). Mice were sacrificed by CO_2 asphyxiation, and hearts were harvested for morphological and histological staining. Statistical analyses were performed using one-way analysis of variance ($p < 0.05$).

Histological Analysis—Hearts were collected, fixed in 4% paraformaldehyde, dehydrated, and embedded in paraffin. Fibrosis was detected with Masson's trichrome staining. The area of collagen deposition in the heart stained by Masson's trichrome (blue) was quantified using Metamorph 6.1 software (Universal Imaging Corp.) as described previously (20). The area occupied by blue pixels was expressed as a percentage of area of the entire heart. Thus the fibrotic area encompasses the scar, border zone, and remote area. A total of three photomicrographs encompassing the entire heart were analyzed for six mice per experimental group. TUNEL staining of apoptotic nuclei following 4 weeks of MI was determined using the fluorescein *in situ* cell death detection kit according to the manufacturer's instructions (Roche Diagnostics) and counterstained with TO-PRO-3 iodine to visualize the nuclei. A minimum of 100,000 myocytes from $n = 6$ animals were analyzed for each experimental group. Anti-cleaved caspase-3 antibody (1:100; catalog no. 9664, Cell Signaling) was used to detect apoptotic cells, and an antibody to 8-hydroxy-2′-deoxyguanosine (8-OHdG) (Oxis International) was used to detect DNA damage in hearts subjected to I/R (3). Immunoreactivity was detected using Pierce ultra-sensitive ABC kit and 3′,3′-diaminobenzidine enhanced metal substrate kit (Pierce). Statistical analyses were performed using Student's *t* test ($p < 0.05$).

Protein Isolation and Western Blotting—Protein lysates were isolated from rat neonatal cardiomyocytes and from

mouse heart ventricles after sham operation or I/R using ice-cold CelLytic MT cell lysis buffer or CelLytic M tissue lysis buffer (Sigma), containing protease inhibitor mixture (Pierce) and phosphatase inhibitor (Pierce) according to the manufacturer's instructions. Western blots were performed as described previously (6). Immunoblots were developed using chemifluorescent detection with the Vistra enhanced chemifluorescence reagent (Amersham Biosciences) and scanned using a Storm 860 (Amersham Biosciences). Signal intensities were quantified with ImageQuant 5.0 software (GE Healthcare). Antibodies used for immunoblot analysis include the following: AMPK (1:1000; catalog no. 2532, Cell Signaling); p-AMPK (1:1000; catalog no. 2535, Cell Signaling); FoxO1 (1:200; catalog no. 2880, Cell Signaling); FoxO3 (1:200; catalog no. 2497, Cell Signaling); phospho-FoxO1 Ser-256 (1:700; catalog no. 9461, Cell Signaling); phospho-FoxO3 Ser-318/321 (1:700; catalog no. 9465, Cell Signaling); LC3 (1:1000; catalog no. 9215, Cell Signaling); ERK (1:1000; catalog no. 9102, Cell Signaling); p-ERK (1:1000; catalog no. 9101, Cell Signaling); Gadd45α (1:1000; catalog no. 3518, Cell Signaling); PINK1 (1:500; catalog no. sc-33796, Santa Cruz Biotechnology); Bcl2 (1:1000; catalog no. sc-7382, Santa Cruz Biotechnology); Bcl-xl (1:1000; catalog no. sc-7195, Santa Cruz Biotechnology); Bax (1:1000; catalog no. sc-493, Santa Cruz Biotechnology), GAPDH (1:10,000; Santa Cruz Biotechnology); catalase (1 μg/ml; catalog no. C0979, Sigma); SOD2 (1 μg/ml; catalog no. 06-984, Millipore); and CITED2 (1:500; catalog no. NB100-136, Novus Biologicals). Statistical significance of observed differences in immunoblot signaling intensities was determined by Student's *t* test ($p < 0.05$, $n = 3–6$).

Quantitative Real Time RT-PCR (qRT-PCR)—Total RNA was isolated from rat neonatal cardiomyocytes or adult mouse hearts for qRT-PCR analysis. 1 μg of total RNA was used to generate cDNA with a Superscript II first strand synthesis kit (Invitrogen) according to the manufacturer's instructions. 1 μl of synthesized cDNA was used for analysis by qRT-PCR (MJ Research Opticon 2) as described previously (6, 21). Oligonucleotide primer sequences used for quantification of mouse *Cat*, *SOD2, Gadd45α*, *PINK1*, *CITED2*, *LC3*, *Gabarapl1,* and *Atg12* were described previously (6, 22–26). Amplification reactions were performed with 34 cycles of (94 °C for 30 s; 55 °C for 45 s; 72 °C for 30 s), and normalized to mRNA expression levels of the ribosomal protein gene *L7* for mouse. Normalized threshold cycle values of samples amplified in triplicate were used to calculate relative gene expression levels. Statistical significance of observed differences was determined by Student's *t* test ($p < 0.05$).

ChIP Assay—DNA-protein complexes isolated from cultured rat neonatal cardiomyocytes subjected to H/R were cross-linked for 10 min by directly adding formaldehyde (Sigma) to the culture medium at a final concentration of 1%. The fixed cells were lysed with lysis buffer (EZ ChIP, Upstate) and sonicated two times for 7 s with output 5 (Virsonic 60; Virtis) with a 2-min refractory period. For immunoprecipitation, cell lysates were incubated with an antibody against FoxO1 (5 μg; Santa Cruz Biotechnology) or FoxO3 (5 μg; Santa Cruz Biotechnology) and incubated overnight at 4 °C. Immunoprecipitation with normal rabbit IgG was used as a negative control. Immunoprecipitation was performed according to the manufacturer's instructions (EZChIP, Upstate), with the exception that protein A-agarose beads were used. The immunoprecipitated and input DNA were subjected to quantitative PCR using SYBR Green PCR reagents and MJ Research Opticon 2 machine with the following primers: *rPINK1,* 5′-GCTACCCCTCCACGGGGTTC-3′ and 5′-GCAGGCCTCGGCCCAGTGCCT-3′; *rCITED2,* 5′-GCAAGTAACTGTGTATGTGCA-3′ and 5′-GTACGTGTGCTTCTGCTAAG-3′ to amplify rat promoter regions containing previously reported FoxO1- and FoxO3-binding sites (22, 25, 27). Fold enrichment relative to IgG antibody control (negative control) was calculated using the comparative C_T method ($\Delta\Delta C_T$) as described previously (28).

Statistical Analysis—Statistical analyses between the experimental groups were performed using a Student's *t* test and one-way analysis of variance. Values of $p < 0.05$ were considered significant.

RESULTS

Induction of Oxidative Stress Either by H/R or Hydrogen Peroxide (H_2O_2) Treatment Results in FoxO Nuclear Localization and Activation of Target Genes—To determine the effect of oxidative stress on endogenous FoxO1 and FoxO3 subcellular localization, cultured neonatal rat cardiomyocytes were subjected to H/R or treated with H_2O_2. Induction of oxidative stress either by H/R or H_2O_2 treatment results in predominant nuclear localization of both FoxO1 and FoxO3 (Fig. 1, *B* and *D, arrows*) indicative of activation, compared with uniform distribution (Fig. 1, *A* and *C*) in normoxic unstressed cardiomyocytes. The levels of phosphorylated AMPK (p-AMPK) over total AMPK were determined during normoxia, H/R, and H_2O_2 treatment. Cardiomyocytes exposed to H/R stress or treated with H_2O_2 demonstrate a significant increase in active AMPK (2-fold with H/R stress and 3.8-fold with H_2O_2 treatment; Fig. 1, *E–G*) compared with the normoxic condition. Likewise, the levels of phosphorylated FoxO1 (p-FoxO1; Ser-256) and phosphorylated FoxO3 (p-FoxO3; Ser-318/321) are significantly decreased with H/R treatment consistent with FoxO activation and nuclear localization (Fig. 1, *E–G*). In addition, protein expression of FoxO targets catalase, SOD2, PINK1, and LC3II all are significantly increased in both H/R and cardiomyocytes treated with H_2O_2 (Fig. 1, *E–G*). Thus oxidative stress promotes nuclear localization of FoxO1 and FoxO3 with increased expression of FoxO targets, including antioxidants and antiapoptotic and autophagy-related genes.

FoxOs Are Necessary and Sufficient to Promote Cardiomyocyte Cell Survival during Oxidative Injury—FoxO gain- and loss-of-function studies were performed in cardiomyocytes to determine the effects of altered FoxO1 and FoxO3 activity on ROS-induced cell death. Cardiomyocytes were infected with recombinant adenoviruses expressing FoxO1(ADA) or FoxO3(TmO3) that lack inactivating AKT phosphorylation sites for constitutive gain-of-function (6). An adenovirus expressing dominant-negative DN-FoxO1(Δ256), which contains the entire forkhead DNA binding domain but lacks the transactivation domain, was used to inhibit all FoxO activity

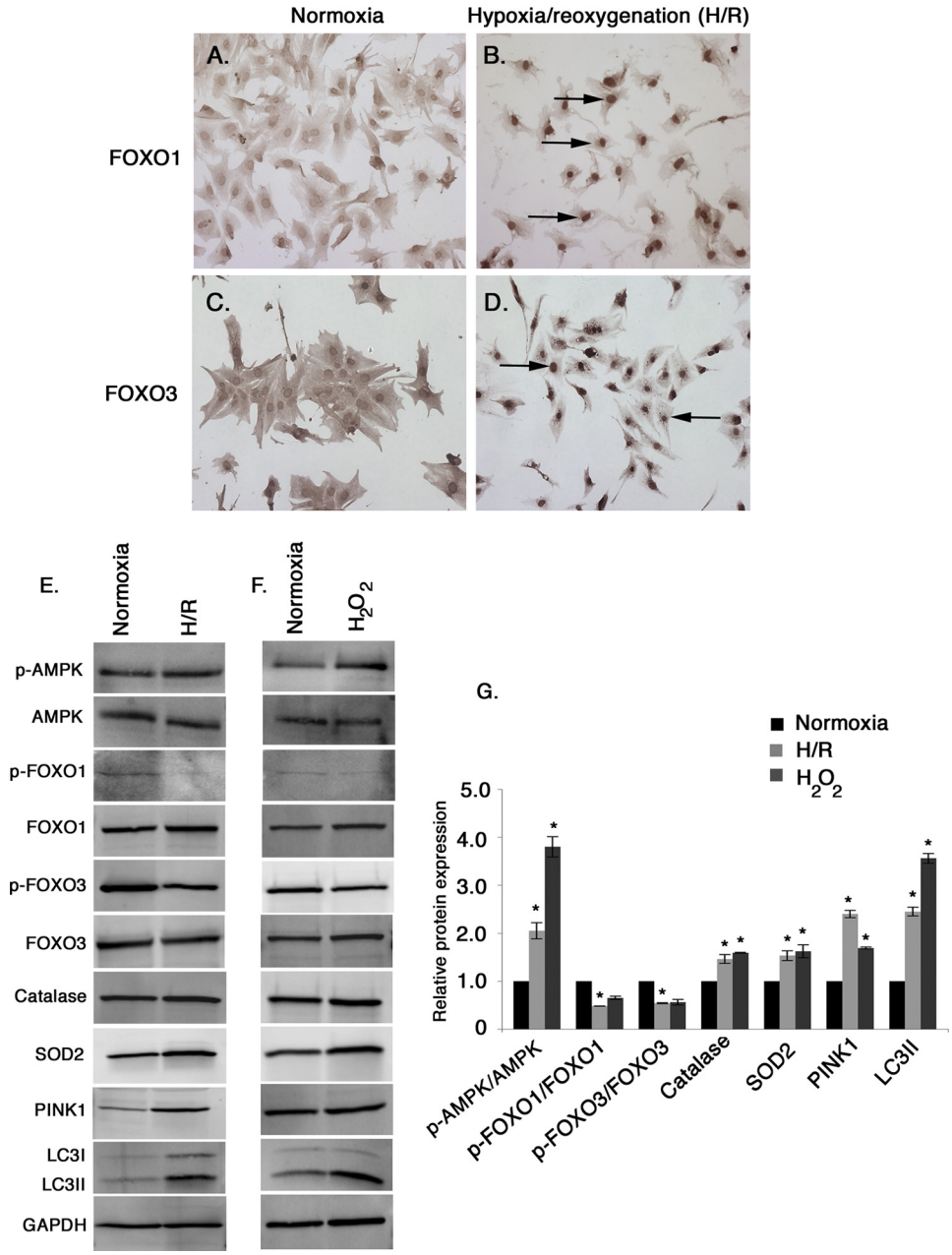

FIGURE 1. **Induction of oxidative stress promotes nuclear localization of endogenous FoxO1 and FoxO3 and activation of FoxO target genes in rat neonatal cardiomyocytes.** *A–D,* neonatal rat cardiomyocytes were subjected to glucose-free hypoxia overnight followed by 5 h of reoxygenation (H/R) (*B* and *D*) compared with control cardiomyocytes cultured in serum containing DMEM (*A* and *C*) (*Normoxia*). Expression and localization of FoxO1 (*A* and *B*) and FoxO3 (*C* and *D*) were determined by immunohistochemistry. Nuclear localization of FoxO1 (*B*) and FoxO3 (*D*) are indicated by *black arrows* in cardiomyocytes subjected to H/R stress. *E–G,* protein expression of p-AMPK/AMPK, p-FoxO1/FoxO1, p-FoxO3/FoxO3, and different FoxO target gene products, catalase, SOD2, PINK1, and LC3II were determined by Western blot and quantified from three independent experiments from normoxic, H_2O_2-treated, and H/R cardiomyocytes. The value of normoxic protein expression is set to 1.0, and the fold change was determined for H/R and H_2O_2-treated cells compared with normoxic condition. Significance was determined by Student's *t* test (*, $p < 0.05$, $n = 3$).

(6). Control cardiomyocytes were infected with CMVβ-galactosidase (β-gal) adenovirus. After 24 h of infection, cardiomyocytes were treated with H_2O_2 to induce oxidative stress. The levels of ROS and the percent (%) TUNEL-positive cells indicative of cell death were determined. Expression of constitutively active FoxO1 or FoxO3 results in significantly decreased H_2O_2-induced cell death (compare Fig. 2, *F* and *G* with *E, arrows*) relative to controls. In contrast, cell death is significantly increased in cardiomyocytes infected with Δ256 DN-FoxO1 (compare Fig. 2*H* with *E, arrows*), as compared with β-gal-infected cells. The quantitative representation of Fig. 2, *A–H,* is shown in Fig. 2*I*. H_2O_2-induced ROS production also is significantly reduced in cardiomyocytes expressing constitutively active FoxO1 or FoxO3, whereas dominant-negative inhibition of FoxOs results in significantly increased production of ROS as compared with β-gal-infected cells (Fig. 2*J*). Thus FoxOs serve to reduce ROS production and appear to provide oxidative defense to a level sufficient to protect cardiomyocytes from oxidative stress-mediated cell death.

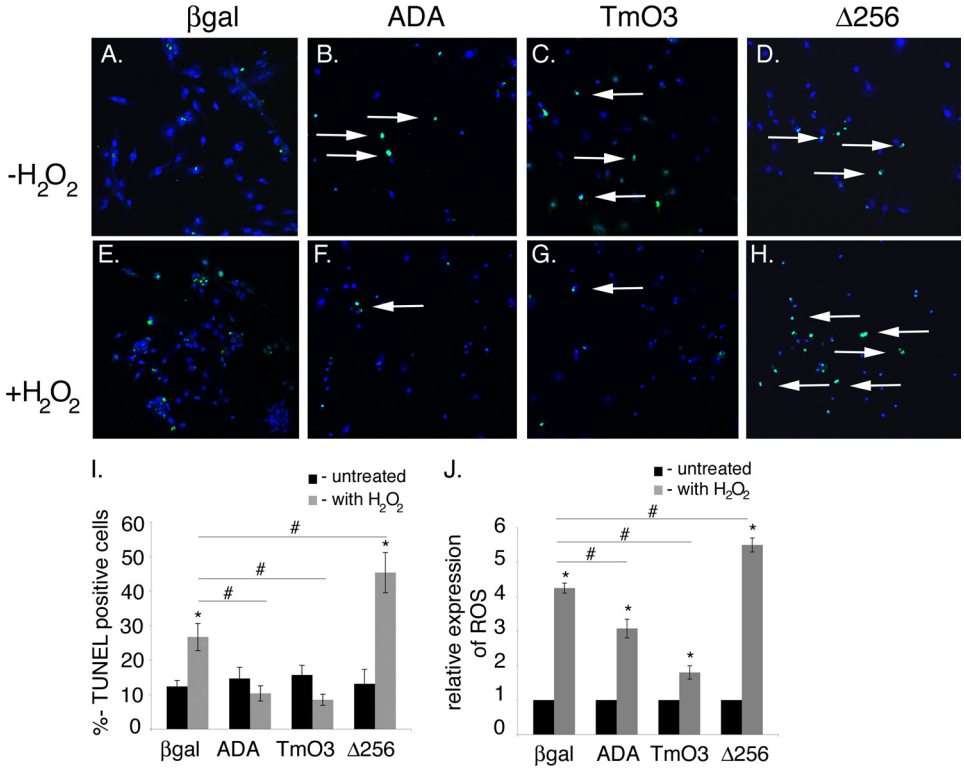

FIGURE 2. **FoxO function is necessary and sufficient to promote cardiomyocyte cell survival during oxidative stress.** *A–J,* neonatal cardiomyocytes were infected with ADA, TmO3, Δ256, or β-galactosidase adenovirus for 24 h and then treated with H_2O_2 for 2 h (*E–H*). Oxidative stress-induced cell death was determined by TUNEL assay (*green* TUNEL-positive cells indicated by *arrows* in *B–D* and *F–H*). *I,* quantitative representation of *A–H*. *J,* oxidative stress-induced ROS production was determined in cardiomyocytes treated with H_2O_2 for 30 min by using the fluorescence marker 2′,7′-dichlorodihydrofluorescein diacetate. Significance was determined by Student's *t* test (*, $p < 0.05$ *versus* without H_2O_2 treatment; #, $p < 0.05$ *versus* β-gal infected with H_2O_2 treatment, $n = 3$).

Combined Deficiency of FoxO1 and FoxO3 Specifically in Cardiomyocytes Results in Increased Cardiac Injury following Acute I/R in Vivo—The ability of FoxOs to protect against oxidative injury in the heart *in vivo* was determined in adult mice with combined deficiency of FoxO1 and FoxO3 specifically in cardiomyocytes. Because both FoxO1 and FoxO3 are expressed in the heart, are activated upon induction of oxidative stress in cardiomyocytes, and are functionally redundant in many cell types, determination of FoxO protective function in the heart *in vivo* necessitates targeting both genes. Mice with targeted insertion of *loxp* sites in the *FoxO1* and *FoxO3* loci have been used previously for Cre-mediated loss-of-function in a variety of cell types (11). Cardiomyocyte-specific loss of FoxO beginning at late fetal stages was achieved by breeding with *βMHC-Cre* mice (29). *βMHC-Cre;FoxO1*$^{fl/fl}$*/FoxO3*$^{fl/fl}$ mice were generated at predicted Mendelian ratios and were apparently normal under base-line conditions. Western blot analysis of heart lysates demonstrates a 70% reduction in FoxO1 and FoxO3 protein levels in *βMHC-Cre;FoxO1*$^{fl/fl}$*/FoxO3*$^{fl/fl}$ mice compared with *FoxO1*$^{fl/fl}$*/FoxO3*$^{fl/fl}$ controls (Fig. 3, *A–C*). To examine FoxO function in regulating cardiomyocyte cell survival upon induction of oxidative stress, mice were subjected to 60-min ischemic injury followed by 24 h of reperfusion, which results in large burst of ROS production. Evan's blue dye and triphenyltetrazolium chloride staining were used to assess the area of myocardial infarction *versus* area at risk. Animals with combined loss of cardiac FoxO1 and FoxO3 (*βMHC-Cre;FoxO1*$^{fl/fl}$*/FoxO3*$^{fl/fl}$) demonstrated a significant increase in infarct area normalized to area at risk (AAR), but no significant changes were observed in AAR compared with the control groups (FVBN wild type (NTG), *βMHC-Cre,* or *FoxO1*$^{fl/fl}$*/FoxO3*$^{fl/fl}$) (Fig. 3, *D* and *E*). Notably, there was no significant difference in infarct area or AAR between NTG and *βMHC-Cre* control animals. Thus cardiac injury following I/R is increased with combined loss of FoxO1 and FoxO3 in cardiomyocytes.

βMHC-Cre;FoxO1$^{fl/fl}$*/FoxO3*$^{fl/fl}$ *Mice Have Increased Susceptibility to Long Term Ischemic Injury*—Mice deficient in cardiac FoxOs were subjected to permanent ligation to examine the long term effects of ischemic injury on ventricular remodeling and cardiac function. The left coronary artery was ligated for 4 weeks, and echocardiographic analysis of heart function was conducted during each subsequent week. After 4 weeks of MI, left ventricular inner dimension at end-systole, indicative of left ventricular chamber dilation, was increased for both *βMHC-Cre;FoxO1*$^{fl/fl}$*/FoxO3*$^{fl/fl}$ and *FoxO1*$^{fl/fl}$*/FoxO3*$^{fl/fl}$, relative to sham-operated controls (Table 1). Furthermore, *βMHC-Cre;FoxO1*$^{fl/fl}$*/FoxO3*$^{fl/fl}$ mice showed significantly greater increases in both left ventricular inner dimension at end-diastole and left ventricular inner dimension at end systole compared with *FoxO1*$^{fl/fl}$*/FoxO3*$^{fl/fl}$ mice after 4 weeks of MI. Thus, FoxO deficiency results in a greater enlargement of the ventricular chamber following MI than is observed in control mice. In addition, *βMHC-Cre;FoxO1*$^{fl/fl}$*/FoxO3*$^{fl/fl}$ mice showed significantly reduced ventricular performance, as indicated by fractional shortening compared

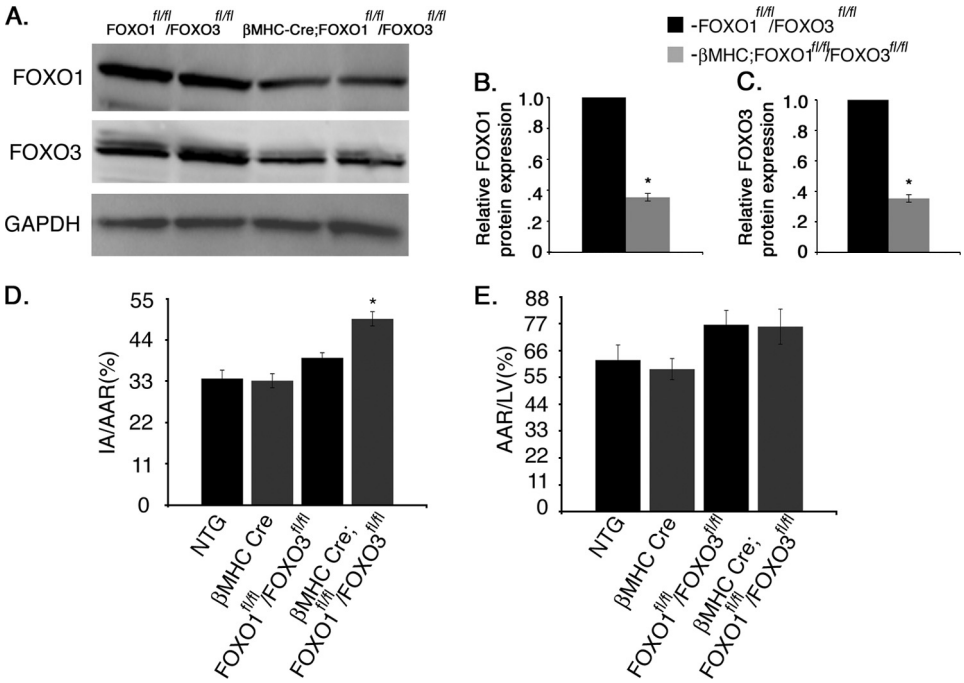

FIGURE 3. **βMHC-Cre;FoxO1$^{fl/fl}$/FoxO3$^{fl/fl}$ mice have increased ischemic injury.** *A,* Western blot assessment of total protein expression of both FoxO1 and FoxO3 in control (*FoxO1$^{fl/fl}$FoxO3$^{fl/fl}$*) and cardiomyocyte-specific FoxO1- and FoxO3-deficient (*βMHC-Cre;FoxO1$^{fl/fl}$/FoxO3$^{fl/fl}$*) mouse hearts. *B* and *C,* quantitative representation of *A* showing 70% reduction of both FoxO1 and FoxO3 in *βMHC-Cre;FoxO1$^{fl/fl}$/FoxO3$^{fl/fl}$* mouse hearts compared with *FoxO1$^{fl/fl}$/FoxO3$^{fl/fl}$* controls. *D* and *E,* NTG, *βMHC-Cre, FoxO1$^{fl/fl}$/FoxO3$^{fl/fl}$*, and *βMHC-Cre;FoxO1$^{fl/fl}$/FoxO3$^{fl/fl}$* mouse hearts were subjected to 1 h of ischemia followed by 24 h of reperfusion and were stained with triphenyltetrazolium chloride and Evan's blue dye to determine cell viability and the area at risk. Quantification of infarct area (*IA*) *versus* AAR shows significant increase in percentage of I/R injury with no significant changes in AAR in *βMHC-Cre;FoxO1$^{fl/fl}$/FoxO3$^{fl/fl}$* compared with NTG, *βMHC-Cre,* and *FoxO1$^{fl/fl}$/FoxO3$^{fl/fl}$* mouse hearts. Significance was determined by Student's *t* test (*, $p < 0.05$; for NTG, $n = 6$, *βMHC-Cre,* $n = 7$, *FoxO1$^{fl/fl}$/FoxO3$^{fl/fl}$*, $n = 7$, and for *βMHC-Cre;FoxO1$^{fl/fl}$/FoxO3$^{fl/fl}$*, $n = 8$).

TABLE 1

Echocardiographic analysis of cardiac structure and function in *FoxO1$^{fl/fl}$/FoxO3$^{fl/fl}$* and *βMHC-Cre;FoxO1$^{fl/fl}$/FoxO3$^{fl/fl}$* mice following 4 weeks of MI or sham operation

The following abbreviations are used: IVSd, interventricular septum at diastole; LVIDd, left ventricular inner diameter at diastole; LVPWd, left ventricular posterior wall thickness at diastole; IVSs, interventricular septum at systole; LVIDs, left ventricular inner diameter at systole; LVPWs, left ventricular posterior wall thickness at systole; MM R-R int, M-mode peak to peak interval; FS, fractional shortening. Statistical significance was determined using one-way analysis of variance.

	FoxO1$^{fl/fl}$/FoxO3$^{fl/fl}$		*βMHC-Cre;FoxO1$^{fl/fl}$/FoxO3$^{fl/fl}$*	
	SHAM ($n = 5$)	MI-4 weeks ($n = 7$)	SHAM ($n = 4$)	MI-4 weeks ($n = 7$)
IVSd	0.08 ± 0.003 cm	0.08 ± 0.002 cm	0.08 ± 0.005 cm	0.08 ± 0.004 cm
LVIDd	0.40 ± 0.012 cm	0.45 ± 0.015 cm	0.38 ± 0.004 cm	0.51 ± 0.010 cm[a,b]
LVPWd	0.09 ± 0.006 cm	0.11 ± 0.004 cm	0.10 ± 0.005 cm	0.09 ± 0.004 cm
IVSs	0.12 ± 0.004 cm	0.13 ± 0.005 cm	0.12 ± 0.004 cm	0.12 ± 0.006 cm
LVIDs	0.26 ± 0.011 cm	0.30 ± 0.017 cm[a]	0.24 ± 0.003 cm	0.39 ± 0.02 cm[a,b]
LVPWs	0.12 ± 0.006 cm	0.13 ± 0.003 cm	0.13 ± 0.006 cm	0.13 ± 0.003 cm
MM R-R int	0.12 ± 0.005	0.13 ± 0.007	0.12 ± 0.004	0.12 ± 0.004
FS	33.3 ± 1.5%	30.0 ± 1.9%	36.0 ± 0.366%	24.1 ± 2.2%[a,b]

[a] $p < 0.05$ sham *versus* MI.
[b] $p < 0.05$ MI *FoxO1$^{fl/fl}$/FoxO3$^{fl/fl}$ versus* MI *βMHC-Cre;FoxO1$^{fl/fl}$/FoxO3$^{fl/fl}$*.

with control mice (Fig. 4*B* and Table 1). Importantly, cardiac function of sham-operated mice from both groups was apparently unaffected, and there was no difference in cardiac function in FoxO-deficient *versus* control mice in the absence of MI (Fig. 4*A* and Table 1). The greater reduction in ventricular performance in *βMHC-Cre;FoxO1$^{fl/fl}$/FoxO3$^{fl/fl}$* mice following MI also is correlated with more extensive scar formation and fibrotic area (2-fold higher) in the left ventricle compared with *FoxO1$^{fl/fl}$/FoxO3$^{fl/fl}$* mice (Fig. 4, *C* and *D*). *βMHC-Cre; FoxO1$^{fl/fl}$/FoxO3$^{fl/fl}$* mice also showed a significant increase in cell death compared with *FoxO1$^{fl/fl}$/FoxO3$^{fl/fl}$* as determined by both TUNEL (3-fold increase) and cleaved caspase-3 (2-fold increase) staining (Fig. 4, *E* and *F*). No significant differences in cell death or fibrotic area were observed between the FoxO-deficient and control mice following sham procedure (Fig. 4, *E* and *F*). Together, these results indicate that combined loss of FoxO1 and FoxO3 in cardiomyocytes leads to increased cell death, increased scar formation, and decreased ventricular performance at 4 weeks post-MI.

Cardiomyocyte-specific Loss of FoxO1 and FoxO3 Results in Increased p38 MAPK Phosphorylation (p-p38) and Altered Expression of Apoptotic Proteins following Acute I/R Injury— Oxidative injury in the heart leads to activation of stress-related signaling pathways, including p38 MAPK, in addition to increased activity of proapoptotic protein Bax and decreased expression of the antiapoptotic protein Bcl-2 (2, 30, 31). These indicators of oxidative stress and apoptosis were examined in cardiomyocyte-specific FoxO-deficient mice subjected

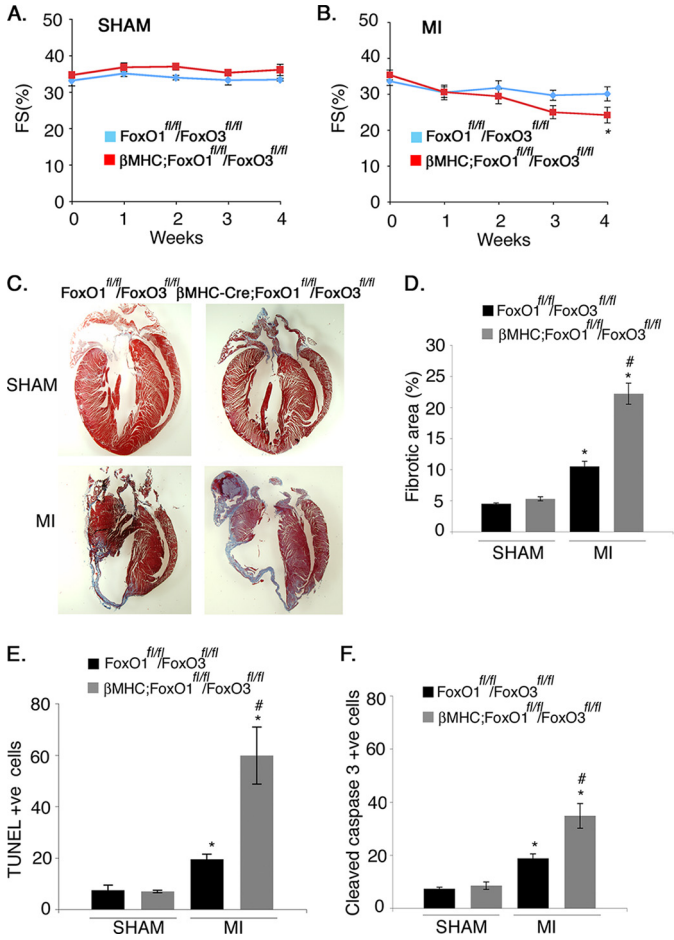

FIGURE 4. **Cardiomyocyte-specific loss of both FoxO1 and FoxO3 leads to increased scar formation and cell death with attenuated cardiac performance following MI.** *A* and *B*, echocardiographic analysis of fractional shortening in *FoxO1*$^{fl/fl}$/*FoxO3*$^{fl/fl}$ and *βMHC-Cre;FoxO1*$^{fl/fl}$/*FoxO3*$^{fl/fl}$ mice subjected to sham or MI surgical procedure for 4 weeks. Statistical significance was determined by one-way analysis of variance (*, $p < 0.05$ *versus* sham, $n = 4–7$). *C*, Masson's trichrome-stained histological sections of hearts from *FoxO1*$^{fl/fl}$/*FoxO3*$^{fl/fl}$ and *βMHC-Cre;FoxO1*$^{fl/fl}$/*FoxO3*$^{fl/fl}$ mice subjected to the sham or MI surgical procedure for 4 weeks. The scar area is shown in *blue*. *D*, quantitative representation of *C* showing significant increased in the percentage of fibrotic area in *βMHC-Cre;FoxO1*$^{fl/fl}$/*FOXO3*$^{fl/fl}$ compared with *FoxO1*$^{fl/fl}$/*FoxO3*$^{fl/fl}$ mice. *E* and *F*, quantitative representation of cell death as determined by the immunohistochemical staining with TUNEL or cleaved caspase-3-specific antibody in *FoxO1*$^{fl/fl}$/*FoxO3*$^{fl/fl}$ and *βMHC-Cre;FoxO1*$^{fl/fl}$/*FoxO3*$^{fl/fl}$ mice subjected to the sham or MI surgical procedure for 4 weeks. Cell death evaluated by both TUNEL (*E*) and cleaved caspase-3 (*F*) is increased in *βMHC-Cre;FoxO1*$^{fl/fl}$/*FoxO3*$^{fl/fl}$ compared with *FoxO1*$^{fl/fl}$/*FoxO3*$^{fl/fl}$ mice. Significance was determined by Student's *t* test (*, $p < 0.05$ *versus* sham and #, $p < 0.05$ *versus* MI, $n = 6$).

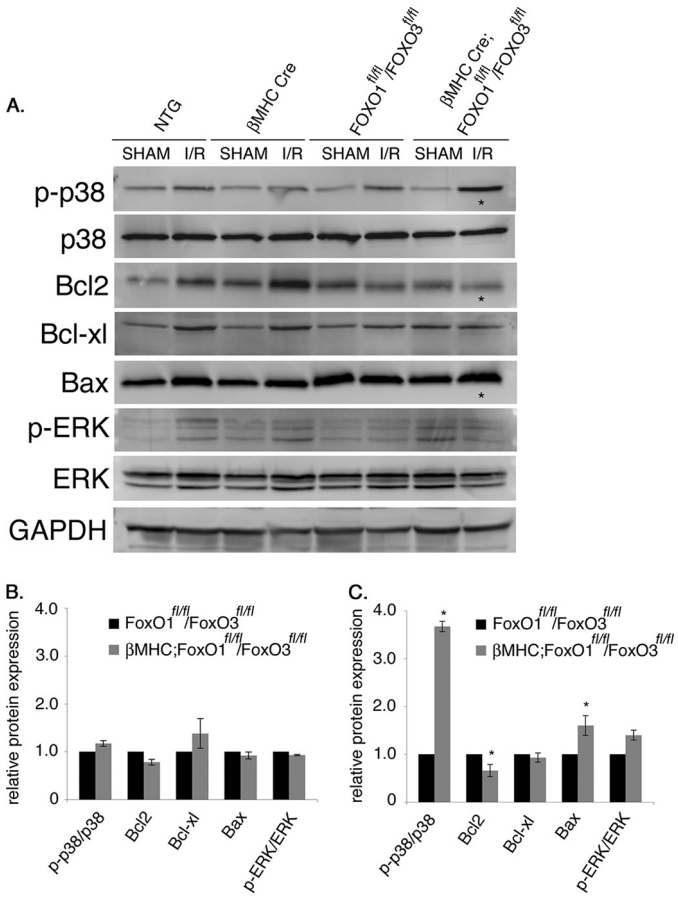

FIGURE 5. **p38 MAPK activation is enhanced in *βMHC-Cre;FoxO1*$^{fl/fl}$/*FoxO3*$^{fl/fl}$ compared with NTG, *βMHC-Cre,* and *FoxO1*$^{fl/fl}$/*FoxO3*$^{fl/fl}$ control mice following acute I/R injury.** *A–C*, Western blot assessment of p38 MAPK signaling, ERK signaling, and apoptotic regulatory proteins in NTG, *βMHC-Cre, FoxO1*$^{fl/fl}$/*FoxO3*$^{fl/fl}$, and *βMHC-Cre;FoxO1*$^{fl/fl}$/*FoxO3*$^{fl/fl}$ hearts following sham operation or acute I/R. The *asterisks* show significant increased p38 phosphorylation (*p-p38*), decreased Bcl2, and increased Bax expression following I/R injury in *βMHC-Cre;FoxO1*$^{fl/fl}$/*FoxO3*$^{fl/fl}$ hearts compared with NTG, *βMHC-Cre,* and *FoxO1*$^{fl/fl}$/*FoxO3*$^{fl/fl}$ controls. No significant changes were observed after the sham procedure among four different genotypes. *B* and *C* are the quantitative representation of protein levels of NTG, *βMHC-Cre, FoxO1*$^{fl/fl}$/*FoxO3*$^{fl/fl}$, and *βMHC-Cre;FoxO1*$^{fl/fl}$/*FoxO3*$^{fl/fl}$ following sham (*B*) and I/R (*C*) procedure. Significance was determined by Student's *t* test (*, $p < 0.05$, $n = 3$).

to 60 min of ischemia followed by 24 h of reperfusion. Strikingly, activated p-p38 over total p38 was increased ~4-fold in *βMHC-Cre;FoxO1*$^{fl/fl}$/*FoxO3*$^{fl/fl}$ mice compared with NTG, *βMHC-Cre,* or *FoxO1*$^{fl/fl}$/*FoxO3*$^{fl/fl}$ control mice following I/R (Fig. 5, *A* and *C*). The expression of anti-apoptotic molecule Bcl2 was significantly reduced, whereas the levels of Bax, a proapoptotic molecule, were significantly increased in *βMHC-Cre;FoxO1*$^{fl/fl}$/*FoxO3*$^{fl/fl}$ compared with NTG, *βMHC-Cre,* or *FoxO1*$^{fl/fl}$/*FoxO3*$^{fl/fl}$ control mice (Fig. 5, *A* and *C*). In contrast, no appreciable activation of ERK signaling pathway was observed between the two groups following I/R injury. As expected, there were no significant changes in the levels of stress-activated kinases or apoptotic proteins in sham-operated animals from different genotypes (Fig. 5, *A* and *B*). The quantitative representation of protein levels after sham procedure for NTG, *βMHC-Cre*, *βMHC-Cre;FoxO1*$^{fl/fl}$/*FoxO3*$^{fl/fl}$, and *FoxO1*$^{fl/fl}$/*FoxO3*$^{fl/fl}$ is shown in Fig. 5*B* and after I/R injury is shown in Fig. 5*C*. Thus, the combined deficiency of FoxO1 and FoxO3 in cardiomyocytes results in increased p-p38 activity, as well as altered Bcl-2 and Bax expression following I/R injury, consistent with increased cell death compared with controls.

Combined Loss of FoxO1 and FoxO3 in Cardiomyocytes Leads to Increased Oxidative Stress and Reduced Expression of Antioxidants, Catalase and SOD2, as well as the DNA Damage Repair Protein Gadd45α following Acute I/R Injury—The extent of oxidative damage and induction of antioxidants was examined in the *βMHC-Cre;FoxO1*$^{fl/fl}$/*FoxO3*$^{fl/fl}$ compared with *FoxO1*$^{fl/fl}$/*FoxO3*$^{fl/fl}$ mouse hearts following acute I/R injury or MI. Myocardial levels of 8-OHdG, a sensitive indicator of oxidative DNA damage, are increased in *βMHC-Cre;*

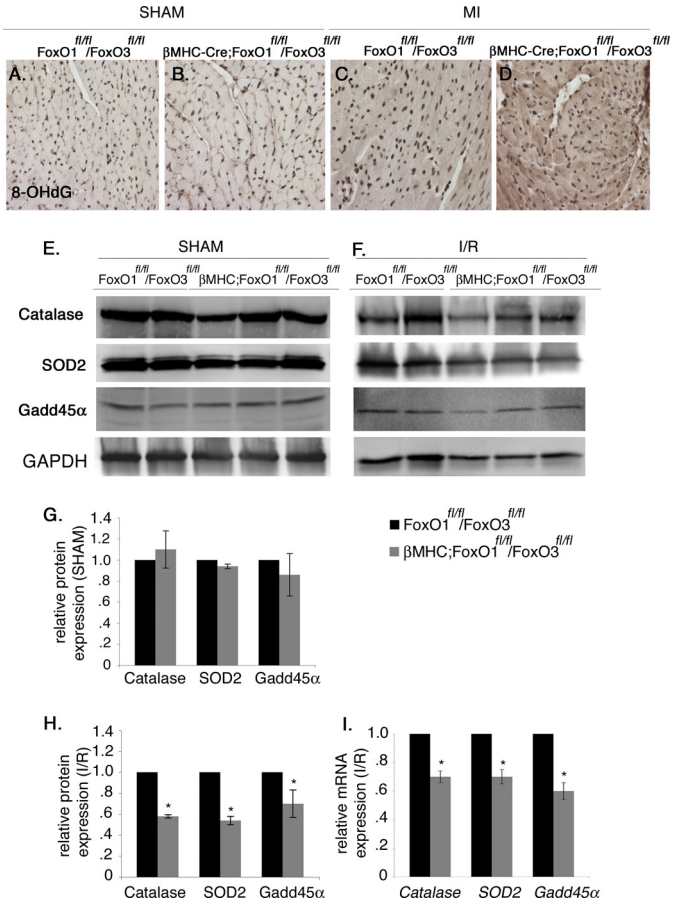

FIGURE 6. **Expression of cardioprotective antioxidants catalase, SOD2, and Gadd45α is decreased in *βMHC-Cre;FoxO1$^{fl/fl}$/FoxO3$^{fl/fl}$* compared with *FoxO1$^{fl/fl}$/FoxO3$^{fl/fl}$* mice following MI and I/R injury.** *A–D,* heart sections were subjected to immunostaining with 8-OHdG, a marker of oxidative DNA damage, which was increased in *βMHC-Cre;FoxO1$^{fl/fl}$/FoxO3$^{fl/fl}$* compared with *FoxO1$^{fl/fl}$/FoxO3$^{fl/fl}$* mice (indicated by *dark brown staining* in *D* compared with *C*), although no noticeable changes were observed after sham procedure (compare *A* and *B*). *E–H,* heart lysates were used to examine the protein expression of catalase, SOD2, and Gadd45α. Immunoblot analyses show a significant decrease in the protein expression of catalase, SOD2, and Gadd45α in *βMHC-Cre;FoxO1$^{fl/fl}$/FoxO3$^{fl/fl}$* compared with *FoxO1$^{fl/fl}$/FoxO3$^{fl/fl}$* mice (*F* and *H*), and no significant changes were observed after the sham procedure (*E* and *G*). *I,* relative gene expression of *Cat*, *SOD2*, and *Gadd45α* was determined by real time qRT-PCR in *βMHC-Cre*; *FoxO1$^{fl/fl}$/FoxO3$^{fl/fl}$* and *FoxO1$^{fl/fl}$/FoxO3$^{fl/fl}$* mice. Significance was determined by Student's *t* test (*, $p < 0.05$; for *FoxO1$^{fl/fl}$/FoxO3$^{fl/fl}$*, $n = 4$, and for *βMHC-Cre;FoxO1$^{fl/fl}$/FoxO3$^{fl/fl}$*, $n = 6$).

FoxO1$^{fl/fl}$/FoxO3$^{fl/fl}$ compared with *FoxO1$^{fl/fl}$/FoxO3$^{fl/fl}$* mice 4 weeks post-MI (Fig. 6, *C* and *D*). Thus, loss of FoxOs in cardiomyocytes is associated with increased oxidative DNA damage after MI. No changes were observed in 8-OHdG reactivity between the two groups in sham-operated animals (Fig. 6, *A* and *B*). The cardioprotective antioxidant genes *SOD2* and *Cat* are direct transcriptional targets of FoxOs and are also induced during I/R (data not shown) (32). *Gadd45α* is a direct downstream target of FoxOs that is induced upon oxidative stress-induced DNA damage as observed during I/R (data not shown) (33, 34). Induction of both protein and mRNA levels of catalase, SOD2, and Gadd45α was significantly reduced in *βMHC-Cre;FoxO1$^{fl/fl}$/FoxO3$^{fl/fl}$* compared with *FoxO1$^{fl/fl}$/FoxO3$^{fl/fl}$* (Fig. 6, *F, H,* and *I*) and *βMHC-Cre* (data not shown) hearts following acute I/R injury. In contrast, no changes in the expression of catalase, SOD2, and Gadd45α were observed between the two groups after the sham procedure (Fig. 6, *E* and *G*). Together, these studies show that the combined loss of FoxO1 and FoxO3 in cardiomyocytes leads to decreased induction of protective antioxidants and DNA repair enzymes associated with increased myocardial damage and cell death following MI or acute I/R injury *in vivo*.

Cardiac-specific FoxO Deficiency Leads to Blunted Induction of Autophagy-related and Antiapoptotic Genes following Acute I/R Injury—Expression of the FoxO target genes *Atg12, Gabarapl1,* and *LC3II*, involved in autophagy, was examined in *βMHC-Cre;FoxO1$^{fl/fl}$/FoxO3$^{fl/fl}$* and *FoxO1$^{fl/fl}$/FoxO3$^{fl/fl}$* mouse hearts subjected to acute I/R. Protein and mRNA expression of LC3II and mRNA expression of *Gabarapl1* in *βMHC-Cre;FoxO1$^{fl/fl}$/FoxO3$^{fl/fl}$* mice are reduced compared with *FoxO1$^{fl/fl}$/FoxO3$^{fl/fl}$* controls following I/R injury (Fig. 7, *B, D* and *E*) with no changes observed in the sham-operated animals (Fig. 7, *A* and *C*). However, no change in *Atg12* gene expression was apparent in *βMHC-Cre;FoxO1$^{fl/fl}$/FoxO3$^{fl/fl}$* and *FoxO1$^{fl/fl}$/FoxO3$^{fl/fl}$* mice subjected to I/R. *PINK1* and *CITED2* are antiapoptotic genes that are direct downstream targets of FoxOs and could be involved in the mechanism for FoxO-mediated protection against oxidative damage in cardiomyocytes (22, 25). Normal FVBN mice subjected to I/R injury show a significant increase in the levels of PINK1 protein expression, although no significant changes were observed in the protein expression of CITED2 compared with sham animals (data not shown). Expression of PINK1 and CITED2 was examined in *βMHC-Cre;FoxO1$^{fl/fl}$/FoxO3$^{fl/fl}$* and *FoxO1$^{fl/fl}$/FoxO3$^{fl/fl}$* mice following I/R injury. Loss of both FoxO1 and FoxO3 in cardiomyocytes results in significant reduction in the protein and mRNA levels of both PINK1 and CITED2 in *βMHC-Cre;FoxO1$^{fl/fl}$/FoxO3$^{fl/fl}$* compared with *FoxO1$^{fl/fl}$/FoxO3$^{fl/fl}$* mice following I/R injury (Fig. 7, *B, D,* and *E*) with no changes in the sham-operated animals (Fig. 7, *A* and *C*). Thus, FoxO deficiency in cardiomyocytes leads to decreased induction of autophagy-related and antiapoptotic genes following acute I/R injury.

ChIP assays were performed to determine whether FoxOs directly bind to the promoter regions of *PINK1* and *CITED2* to transcriptionally regulate expression in neonatal cardiomyocytes. In mouse embryonic fibroblast cultures, FoxO3 directly binds to the promoter regions of both *PINK1* and *CITED2*, but the binding of FoxO1 to the promoter region of these genes or FoxO binding in cardiomyocytes has not been reported previously (22, 25). The region amplified from the promoter region of rat *PINK1* is 49% identical to the corresponding mouse promoter region and contains a conserved FoxO consensus DNA-binding site "GTTGTTGT." Similarly, the amplified region of the rat *CITED2* promoter is 100% identical to the corresponding mouse promoter and contains the conserved FoxO consensus DNA-binding site "AAACAA." Upon induction of oxidative stress, both FoxO1 and FoxO3 are able to bind the identified promoter regions of *PINK1* and *CITED2* in neonatal cardiomyocytes with 4- and 12-fold enrichment in amplification after immunoprecipitation, respectively, over IgG antibody control (Fig. 7, *F–H*). Together, these data suggest that FoxO transcription factors are activated dur-

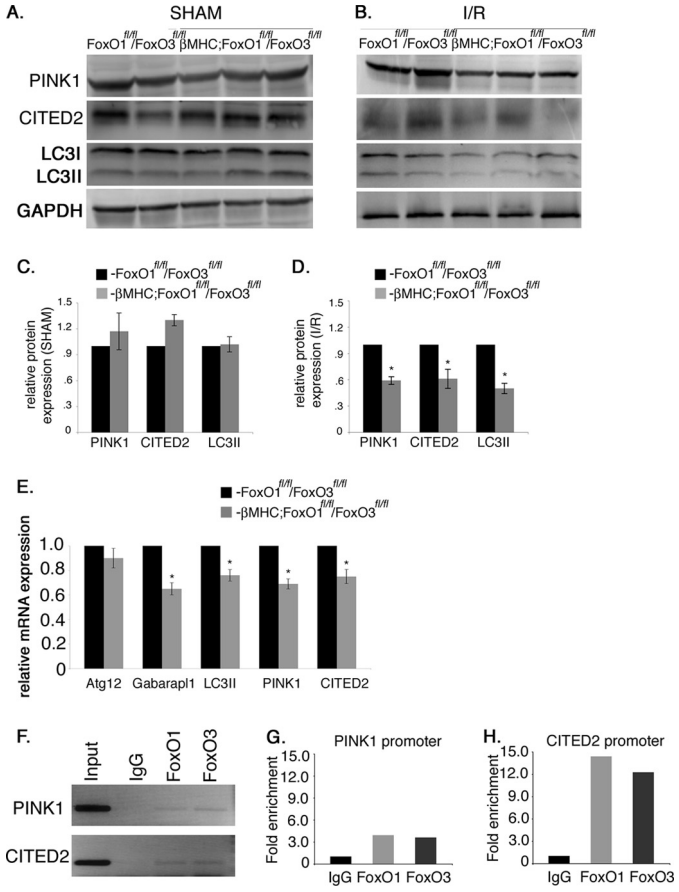

FIGURE 7. **Expression of anti-apoptotic and autophagy-related genes are decreased in *βMHC-Cre*;*FoxO1*$^{fl/fl}$/*FoxO3*$^{fl/fl}$ compared with *FoxO1*$^{fl/fl}$/*FoxO3*$^{fl/fl}$ mice following I/R injury.** *A–D,* heart lysates were used to examine the protein expression of anti-apoptotic proteins PINK1, CITED2, and an autophagy-related protein LC3II. Immunoblot analyses show a significant decrease in the protein expression of PINK1, CITED2, and LC3II in *βMHC-Cre*;*FoxO1*$^{fl/fl}$/*FoxO3*$^{fl/fl}$ compared with FoxO1$^{fl/fl}$/FoxO3$^{fl/fl}$ mice (*B*) with no significant changes observed after sham procedure (*A*). *C* and *D* are the quantitative representation of *A* and *B,* respectively. *E,* relative gene expression of *PINK1, CITED2, LC3II, ATG12,* and *Gabarapl1* was determined by real time qRT-PCR in *βMHC-Cre*;*FoxO1*$^{fl/fl}$/*FoxO3*$^{fl/fl}$ and *FoxO1*$^{fl/fl}$/*FoxO3*$^{fl/fl}$ mice. Significance was determined by Student's *t* test (*, $p < 0.05$; for *FoxO1*$^{fl/fl}$/*FoxO3*$^{fl/fl}$, $n = 4$, and for *βMHC-Cre*;*FoxO1*$^{fl/fl}$/*FoxO3*$^{fl/fl}$, $n = 6$). *F,* ChIP assay demonstrates that both FoxO1 and FoxO3 bind to the promoter regions of PINK1 and CITED2 under H/R conditions. *G* and *H,* graphs are fold enrichment relative to background (IgG antibody control) as determined by qPCR.

ing oxidative stress to directly regulate the expression of two antiapoptotic factors, *PINK1* and *CITED2*. Therefore, the reduced expression of *PINK1* and *CITED2* observed with cardiomyocyte FoxO deficiency likely contributes to the increased cell death and attenuated cardiac performance seen in *βMHC-Cre*;*FoxO1*$^{fl/fl}$/*FoxO3*$^{fl/fl}$ mice compared with *FoxO1*$^{fl/fl}$/*FoxO3*$^{fl/fl}$ mice following acute I/R injury or long term MI.

DISCUSSION

FoxOs regulate diverse cellular functions, including proliferation, apoptosis, DNA repair, defense against oxidative stress, and autophagy, depending on the cellular environment in many cell types (35). Here, we show that oxidative stress in cardiomyocytes promotes nuclear localization of both FoxO1 and FoxO3 and subsequent activation of FoxO target genes with cardioprotective functions. In cultured cardiomyocytes, increased FoxO function leads to decreased cell death, decreased production of ROS, and increased expression of antioxidants, autophagy-related genes, and antiapoptotic proteins. In mice, combined deficiency of FoxO1 and FoxO3 specifically in cardiomyocytes results in increased myocardial cell death, reduced cardiac performance, and increased scar formation following MI. Increased cardiac I/R injury in mice with cardiac FoxO deficiency is accompanied by reduced expression of antioxidants, DNA repair enzymes, autophagy-related genes, and antiapoptotic genes. Conversely, the p38 stress signaling pathway is induced, and expression of apoptotic regulatory proteins Bcl-2 and Bax are altered consistent with the observed increased in cell death. Together, these data show that FoxOs promote oxidative stress resistance in cardiomyocytes through activation of antioxidant, antiapoptotic, and autophagy-related genes.

Oxidative stress activates FoxOs in different cell types mediated by AMPK and sirtuins (class III histone deacetylases, Sirt1 and Sirt3) (3, 23, 24). In the heart, AMPK is an important sensor and regulator of cellular energy status that responds to energy depletion by stimulating ATP production (36). AMPK also is activated in response to I/R injury, resulting in decreased intracellular ROS levels and protection of cardiomyocytes from oxidative damage (4, 37). In cultured fibroblasts, AMPK-mediated activation of FoxOs leads to increased expression of several genes that are important for controlling energy balance and oxidative stress resistance (23). Likewise, Sirt1 and Sirt3 are activated upon induction of oxidative stress and are protective from oxidative damage through induction of antioxidants SOD2 and catalase in the heart (3, 24). The current finding that FoxOs are necessary for induction of antioxidant gene expression and protection against oxidative injury is consistent with their being critical transcriptional mediators of AMPK and Sirt-mediated cardiac protection.

This study supports a mechanism for FoxO-mediated cardioprotection through activation of antioxidant, antiapoptotic, and autophagy genes during conditions of oxidative stress. The antioxidants catalase and SOD2 reduce I/R-induced pathophysiology and are direct downstream targets of FoxOs in cardiomyocytes (38, 39). The antiapoptotic gene *CITED2* also is activated by FoxOs in cardiomyocytes, and FoxO3 inhibits HIF1-induced apoptosis by directly stimulating the transcription of *CITED2* in fibroblasts under hypoxic conditions (22). Likewise PINK1 is a direct downstream target of FoxOs that regulates the anti-oxidative stress response and is activated by FoxO3 as a cell survival mechanism during cytokine deprivation (25). Gadd45α, a DNA repair protein, is a FoxO direct downstream target that is up-regulated in rat hearts following exposure to paraquat, an inducer of oxidative stress (33, 34). Recently we have demonstrated that FoxOs directly regulate the transcription of the autophagy-related genes *Atg12* and *Gabarapl1* in cardiomyocytes under starvation conditions (6). Here, we demonstrate that induction of autophagy-related genes also is dependent on FoxO function during cardiac I/R. Autophagy is induced by ischemic precon-

ditioning and is essential for cardioprotection following oxidative injury (40). Therefore, the protective effects of FoxOs during oxidative injury appear to be multifactorial through inhibition of ROS production, inhibition of apoptosis, and induction of autophagy.

Several factors, including AMPK, Sirt1 and −3, HIF1-α, and miR199a, have been implicated as high level regulators of cardioprotection during oxidative injury (3, 37, 41, 42). Among these, AMPK has emerged as an important signaling molecule in the induction of cardioprotection in I/R injury, and mutations in human AMPK genes have been associated with cardiac dysfunction and hypertrophy (4, 43). Here, we demonstrate that the AMPK-regulated transcription factors FoxO1 and FoxO3 are necessary and sufficient to promote cardiomyocyte cell survival under conditions of oxidative stress. In addition, this cardioprotective effect is associated with increased expression of antioxidant, antiapoptotic, and autophagy-related genes known to be direct downstream targets of FoxOs in multiple cell types. Together these findings support a critical role for FoxOs in limiting ROS production and cell death in response to I/R injury in the heart. However, both AMPK and FoxOs have pleiotropic functions in the regulation of cardiomyocyte metabolism and cell proliferation in response to a variety of stresses, including hypoxia, starvation, and pressure overload. Therefore, it remains to be seen if manipulation of AMPK or FoxO function of specific FoxO downstream targets in the heart will be an effective therapeutic approach in the treatment of cardiovascular disease.

Acknowledgments—We thank Michelle Sargent for performance of cardiac ischemia and myocardial infarction in mice, Allen York for performing the echocardiographic analysis in mice, and Christina Alfieri for technical support.

REFERENCES

1. Murphy, E., and Steenbergen, C. (2008) *Physiol. Rev.* **88,** 581–609
2. Finkel, T., and Holbrook, N. J. (2000) *Nature* **408,** 239–247
3. Alcendor, R. R., Gao, S., Zhai, P., Zablocki, D., Holle, E., Yu, X., Tian, B., Wagner, T., Vatner, S. F., and Sadoshima, J. (2007) *Circ. Res.* **100,** 1512–1521
4. Wang, Y., Gao, E., Tao, L., Lau, W. B., Yuan, Y., Goldstein, B. J., Lopez, B. L., Christopher, T. A., Tian, R., Koch, W., and Ma, X. L. (2009) *Circulation* **119,** 835–844
5. Evans-Anderson, H. J., Alfieri, C. M., and Yutzey, K. E. (2008) *Circ. Res.* **102,** 686–694
6. Sengupta, A., Molkentin, J. D., and Yutzey, K. E. (2009) *J. Biol. Chem.* **284,** 28319–28331
7. Castrillon, D. H., Miao, L., Kollipara, R., Horner, J. W., and DePinho, R. A. (2003) *Science* **301,** 215–218
8. Hosaka, T., Biggs, W. H., 3rd., Tieu, D., Boyer, A. D., Varki, N. M., Cavenee, W. K., and Arden, K. C. (2004) *Proc. Natl. Acad. Sci. U.S.A.* **101,** 2975–2980
9. Ni, Y. G., Berenji, K., Wang, N., Oh, M., Sachan, N., Dey, A., Cheng, J., Lu, G., Morris, D. J., Castrillon, D. H., Gerard, R. D., Rothermel, B. A., and Hill, J. A. (2006) *Circulation* **114,** 1159–1168
10. Greer, E. L., and Brunet, A. (2005) *Oncogene* **24,** 7410–7425
11. Paik, J. H., Kollipara, R., Chu, G., Ji, H., Xiao, Y., Ding, Z., Miao, L., Tothova, Z., Horner, J. W., Carrasco, D. R., Jiang, S., Gilliland, D. G., Chin, L., Wong, W. H., Castrillon, D. H., and DePinho, R. A. (2007) *Cell* **128,** 309–323
12. De Windt, L. J., Lim, H. W., Haq, S., Force, T., and Molkentin, J. D. (2000) *J. Biol. Chem.* **275,** 13571–13579
13. Tokudome, S., Sano, M., Shinmura, K., Matsuhashi, T., Morizane, S., Moriyama, H., Tamaki, K., Hayashida, K., Nakanishi, H., Yoshikawa, N., Shimizu, N., Endo, J., Katayama, T., Murata, M., Yuasa, S., Kaneda, R., Tomita, K., Eguchi, N., Urade, Y., Asano, K., Utsunomiya, Y., Suzuki, T., Taguchi, R., Tanaka, H., and Fukuda, K. (2009) *J. Clin. Invest.* **119,** 1477–1488
14. Nakae, J., Kitamura, T., Silver, D., and Accili, D. (2001) *J. Clin. Invest.* **108,** 1359–1367
15. Skurk, C., Maatz, H., Kim, H. S., Yang, J., Abid, M. R., Aird, W. C., and Walsh, K. (2004) *J. Biol. Chem.* **279,** 1513–1525
16. Wu, C., Yan, L., Depre, C., Dhar, S. K., Shen, Y. T., Sadoshima, J., Vatner, S. F., and Vatner, D. E. (2009) *Am. J. Physiol. Cell Physiol.* **297,** C928–C934
17. Oka, T., Maillet, M., Watt, A. J., Schwartz, R. J., Aronow, B. J., Duncan, S. A., and Molkentin, J. D. (2006) *Circ. Res.* **98,** 837–845
18. De Windt, L. J., Lim, H. W., Taigen, T., Wencker, D., Condorelli, G., Dorn, G. W., 2nd, Kitsis, R. N., and Molkentin, J. D. (2000) *Circ. Res.* **86,** 255–263
19. Kaiser, R. A., Bueno, O. F., Lips, D. J., Doevendans, P. A., Jones, F., Kimball, T. F., and Molkentin, J. D. (2004) *J. Biol. Chem.* **279,** 15524–15530
20. Maillet, M., Lynch, J. M., Sanna, B., York, A. J., Zheng, Y., and Molkentin, J. D. (2009) *J. Clin. Invest.* **119,** 3079–3088
21. Shelton, E. L., and Yutzey, K. E. (2007) *Dev. Biol.* **302,** 376–388
22. Bakker, W. J., Harris, I. S., and Mak, T. W. (2007) *Mol. Cell* **28,** 941–953
23. Greer, E. L., Oskoui, P. R., Banko, M. R., Maniar, J. M., Gygi, M. P., Gygi, S. P., and Brunet, A. (2007) *J. Biol. Chem.* **282,** 30107–30119
24. Sundaresan, N. R., Samant, S. A., Pillai, V. B., Rajamohan, S. B., and Gupta, M. P. (2008) *Mol. Cell. Biol.* **28,** 6384–6401
25. Mei, Y., Zhang, Y., Yamamoto, K., Xie, W., Mak, T. W., and You, H. (2009) *Proc. Natl. Acad. Sci. U.S.A.* **106,** 5153–5158
26. Zhao, J., Brault, J. J., Schild, A., Cao, P., Sandri, M., Schiaffino, S., Lecker, S. H., and Goldberg, A. L. (2007) *Cell Metab.* **6,** 472–483
27. Barthel, A., Schmoll, D., and Unterman, T. G. (2005) *Trends Endocrinol. Metab.* **16,** 183–189
28. Mandel, E. M., Kaltenbrun, E., Callis, T. E., Zeng, X. X., Marques, S. R., Yelon, D., Wang, D. Z., and Conlon, F. L. (2010) *Development* **137,** 1919–1929
29. Parsons, S. A., Millay, D. P., Wilkins, B. J., Bueno, O. F., Tsika, G. L., Neilson, J. R., Liberatore, C. M., Yutzey, K. E., Crabtree, G. R., Tsika, R. W., and Molkentin, J. D. (2004) *J. Biol. Chem.* **279,** 26192–26200
30. Hochhauser, E., Kivity, S., Offen, D., Maulik, N., Otani, H., Barhum, Y., Pannet, H., Shneyvays, V., Shainberg, A., Goldshtaub, V., Tobar, A., and Vidne, B. A. (2003) *Am. J. Physiol. Heart Circ. Physiol.* **284,** H2351–H2359
31. Chen, Z., Chua, C. C., Ho, Y. S., Hamdy, R. C., and Chua, B. H. (2001) *Am. J. Physiol. Heart Circ. Physiol.* **280,** H2313–H2320
32. Jin, Z. Q., Zhou, H. Z., Cecchini, G., Gray, M. O., and Karliner, J. S. (2005) *Am. J. Physiol. Heart Circ. Physiol.* **288,** H2986–H2994
33. Tran, H., Brunet, A., Grenier, J. M., Datta, S. R., Fornace, A. J., Jr., DiStefano, P. S., Chiang, L. W., and Greenberg, M. E. (2002) *Science* **296,** 530–534
34. Edwards, M. G., Sarkar, D., Klopp, R., Morrow, J. D., Weindruch, R., and Prolla, T. A. (2003) *Physiol. Genomics* **13,** 119–127
35. Calnan, D. R., and Brunet, A. (2008) *Oncogene* **27,** 2276–2288
36. Li, X. N., Song, J., Zhang, L., LeMaire, S. A., Hou, X., Zhang, C., Coselli, J. S., Chen, L., Wang, X. L., Zhang, Y., and Shen, Y. H. (2009) *Diabetes* **58,** 2246–2257
37. Russell, R. R., 3rd., Li, J., Coven, D. L., Pypaert, M., Zechner, C., Palmeri, M., Giordano, F. J., Mu, J., Birnbaum, M. J., and Young, L. H. (2004) *J. Clin. Invest.* **114,** 495–503
38. Kops, G. J., Dansen, T. B., Polderman, P. E., Saarloos, I., Wirtz, K. W., Coffer, P. J., Huang, T. T., Bos, J. L., Medema, R. H., and Burgering,

B. M. (2002) *Nature* **419,** 316–321
39. Tan, W. Q., Wang, K., Lv, D. Y., and Li, P. F. (2008) *J. Biol. Chem.* **283,** 29730–29739
40. Huang, C., Yitzhaki, S., Perry, C. N., Liu, W., Giricz, Z., Mentzer, R. M., and Gottlieb, R. A. (2010) *J. Cardiovasc. Trans. Res.* **4,** 365–373
41. Rane, S., He, M., Sayed, D., Vashistha, H., Malhotra, A., Sadoshima, J., Vatner, D. E., Vatner, S. F., and Abdellatif, M. (2009) *Circ. Res.* **104,** 879–886
42. Eckle, T., Köhler, D., Lehmann, R., El Kasmi, K., and Eltzschig, H. K. (2008) *Circulation* **118,** 166–175
43. Arad, M., Seidman, C. E., and Seidman, J. G. (2007) *Circ. Res.* **100,** 474–488